Journal of Structural Geology, Vol. 7, No. 5, pp. 527 to 539, 1985
Printed in Great Britain

0191-8141/85 $03.00 + 0.00

Plagioclase microfabrics in a ductile shear zone from the Jotun Nappe, Norway

LARS N. JENSEN

Statoil A/S, Postboks 40, N-9401 Harstad, Norway

and

JOHN STARKEY

Department of Geology, University of Western Ontario, London, Ont. N6A 5B7, Canada

(*Received* 30 *March* 1984; *accepted in revised form* 12 *November* 1984)

Abstract—Gabbroic and anorthositic rocks from the Jotun Nappe are transected by small ductile shear zones in which a high-grade paragenesis and a new foliation are formed. Most plagioclase grains show evidence of plastic deformation, and have recrystallized by subgrain rotation and 'bulge' processes to fine-grained mylonite. During these processes a plagioclase grain-shape fabric was destroyed, and with increasing strain a pre-existing plagioclase crystal fabric was successively modified, enhanced and finally obliterated. This could be evidence of superplastic flow. Inverse pole figure analysis of the typical plagioclase crystal fabric in the shear zone indicates that (021) $\perp\langle a\rangle$ could be an operative slip system, and planes close to (132) could be possible slip planes.

INTRODUCTION

ALTHOUGH the literature on feldspar chemistry and crystal structure is extensive, relatively little research has focused on the relations between plastic deformation, dynamic recrystallization and microfabric of these minerals. In contrast, the last decade has seen a dramatic increase in the study of the microfabrics of deformed quartz, calcite and olivine, especially in relation to the development of ductile shear zones. The observations from these studies are used here to provide a strategy for similar studies of plagioclase.

In any study of the relations between deformation and microfabric of plagioclase, it is desirable to have a well-defined and localized deformation event in a rock rich in plagioclase. This analysis is based on a specimen from a small shear zone in the gabbroic and anorthositic gneisses of the Jotun Nappe, Norway (Fig. 1a).

STRUCTURES AND MICROSTRUCTURES

The Jotun Nappe is the highest member of the Caledonian thrust pile in Southern Norway. The thrust sheet is composed of an upper and lower unit, commonly with a tectonic contact between them (Fig. 1b). The upper unit consists largely of layered metamorphic rocks of granodioritic, gabbroic and anorthositic composition (Bryhni *et al.* 1983, fig. 2). We refer to the layering as S_L.

Two generations of ductile shear zones cut across the layering of the upper unit (Heim *et al.* 1977, N. Ø. Olesen pers. comm.). The youngest set is related to the thrusting and caused retrogression of the gneisses to the greenschist facies. An older set of small-scale shear zones, generally less than 2 m wide, shows a high-grade paragenesis and was formed during a metamorphic episode prior to the emplacement of the nappe. The sample described here is from the margin of one of these high-grade ductile shear zones (Fig. 2). Figure 1(b) shows the sample location and presents a general view of the geology of the southern part of the Jotun Nappe. A detailed description of the geology of that area has been given by Bryhni *et al.* (1983).

The sample has a gabbroic to anorthositic composition (Table 1a) according to the classification system of Buddington (1939). The stable paragenesis is plagioclase (An_{68-78}), amphibole and garnet, and neither the modal percentages of the minerals (Table 1b), the composition of the minerals nor the stable paragenesis change across the shear zone. Similar shear zones from the Jotun Nappe are described by Bryhni *et al.* (NGU Internal Report No. 1560/28, 1977) and Boullier & Gueguen (1975), who suggest a temperature of about 600°C during the shear zone development.

Mesoscopic structures

The sample contains the margin of a 10–15 cm wide shear zone which cross cuts the layered gneisses (Figs. 2 and 3a). Based on the structures and microstructures, and for convenience of further description, the sample is divided into three zones described below.

Zone I. The layered gneisses are grey to light grey and medium grained. Dark layers are 0.5–2 cm thick and have a gabbroic to amphibolitic composition, whereas light layers are 5–10 cm thick and have an anorthositic composition. Clusters of amphibole grains, 0.5–2 cm long, occur in the anorthositic layers and are commonly elongate and lie parallel to the layering. Many of these clusters form a corona structure (Spry 1969) around garnet grains.

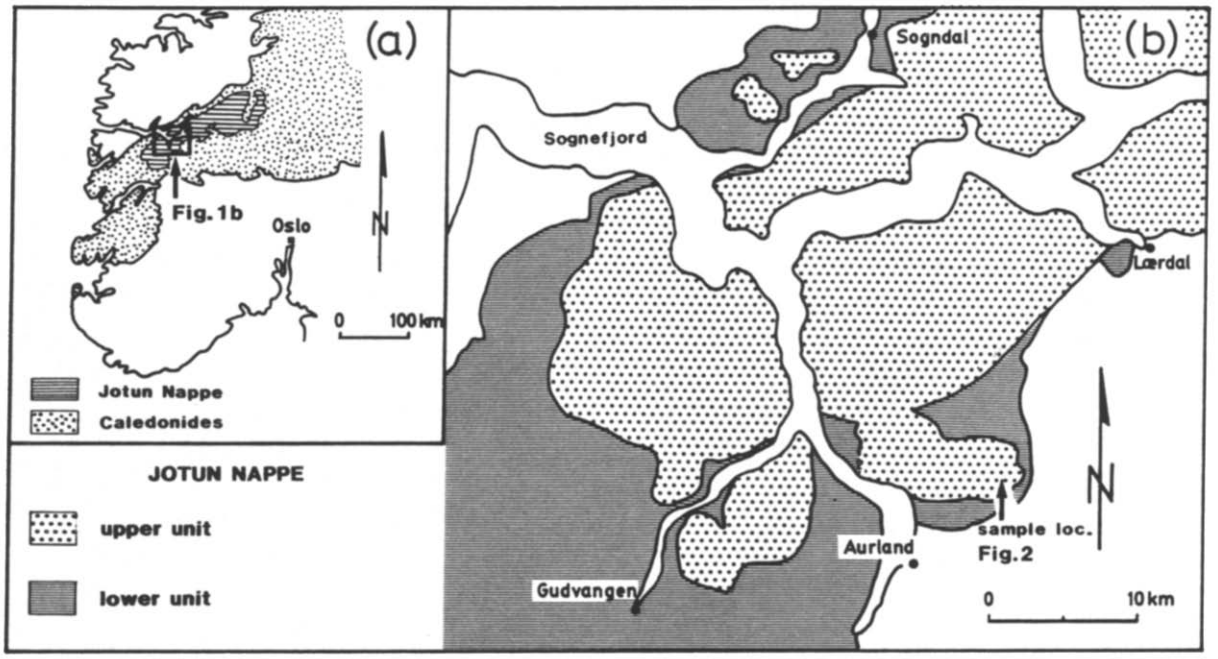

Fig. 1.(a) Geological map of southern Norway showing the location of the Jotun Nappe. (b) Simplified geological map of the south western part of the Jotun Nappe (after Bryhni *et al.* NGU Internal Report No. 1560/28, 1977) with the sample location (60°57′9″N, 6°19′47″E).

Zone II. Across a 3–5 cm wide zone, the layering has been progressively rotated towards parallelism with the boundary of the shear zone, and a new foliation (S_M) becomes visible. The new foliation is defined by the shape fabric of clusters of amphibole. As the angle between the new foliation and the boundary of the shear zone decreases, the aspect ratio and shape fabric of the amphibole clusters increase, the spacing between S_M planes decreases and the new foliation becomes dominant (Fig. 3a). Zone II grades into zone III within a distance of less than 3 mm. Mylonitic folia starting in zone II can be traced into zone III, and the angle between the boundary of the shear zone and these mylonitic folia is used to calculate the shear strain (Ramsay & Graham 1970), as shown in Fig. 3(c).

Zone III. The sheared gneisses are dark grey and fine-grained, with a distinct mylonitic foliation (S_M). The original compositional layering (S_L) is completely obliterated and the new foliation is subparallel to the shear zone.

The sample used in this study was cut perpendicular to the boundary of the shear zone and within 10° of the shear direction. This direction is not well defined, as the shear zone shows no associated linear structures; but by viewing the rotation of S_L and S_M on three faces of the sample, an estimate of the shear direction was made. The contact plane between zones II and III (Fig. 3b) is used as reference plane throughout this paper, and is regarded as being parallel to the shear plane.

Microstructures

The three zones described above coincide with three distinct microstructural zones defined by the texture of plagioclase and amphibole (Fig. 4). The microstructural nomenclature used here follows that of Kehlenbeck (1972) and Brown *et al.* (1980).

Zone I. The layered gneisses have a porphyroclastic mortar texture of residual grains surrounded by multiple walls of new grains (Figs. 4a and 5a). The old and the new grains each constitute about 50% by volume. The residual grains are 0.5–4 mm in diameter, with a mean of about 2 mm. They are equant to slightly elongate in shape, with lobate but smooth and well-defined grain boundaries. All residual grains show polysynthetic twinning and evidence of strain, such as bent and deformed twins, undulatory extinction and narrow needle-shaped twins terminating inside the grains. Many grains show subgrains and bands with differing extinction, but kink bands are rare. Where residual grains are in contact, their mutual boundaries are lobate and may contain a few small recrystallised grains (Fig. 5b). Some residual grains show embayments by new grains (Fig. 5c); others are completely cross-cut by a layer of new grains.

The recrystallized grains are 0.05–0.5 mm in diameter, with a mean around 0.2 mm. Their shape is equant to slightly elongate, with curved to lobate grain boundaries. Locally the recrystallized grains form a low-energy equilibrium microstructure, but normally their texture is more irregular and many grains show evidence of strain. About 30% of the new grains, usually the smaller ones, are optically twin-free.

Zone II. The plagioclase grains range from 0.02 to 1.5 mm in diameter, and the grain-size distribution is not bimodal as in zone I. The general microstructure of plagioclase is an inequigranular mosaic of lobate grains (Figs. 4a & b and 5d). Only a few (less than 5% by

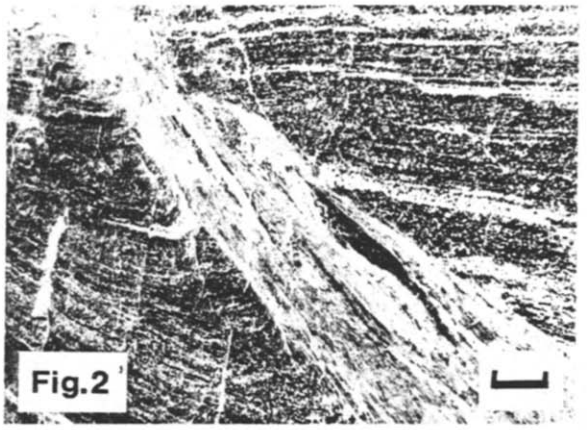

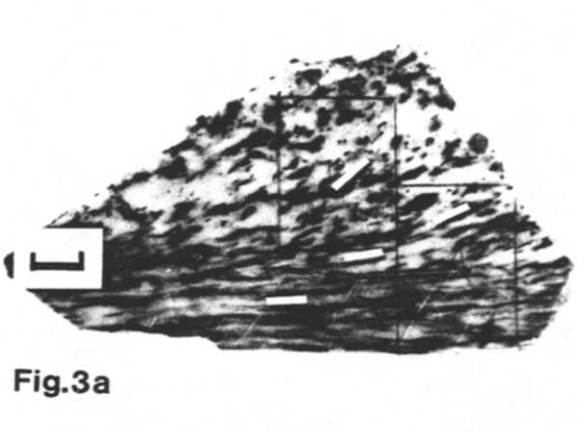

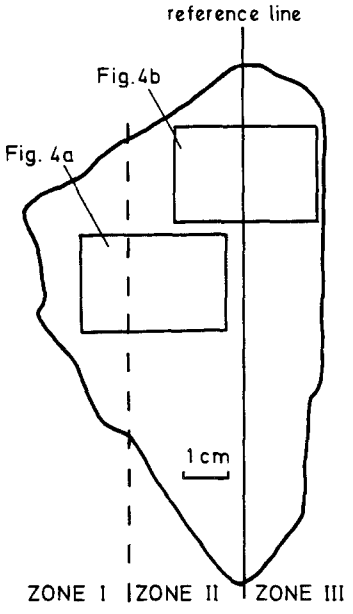

Fig.3b

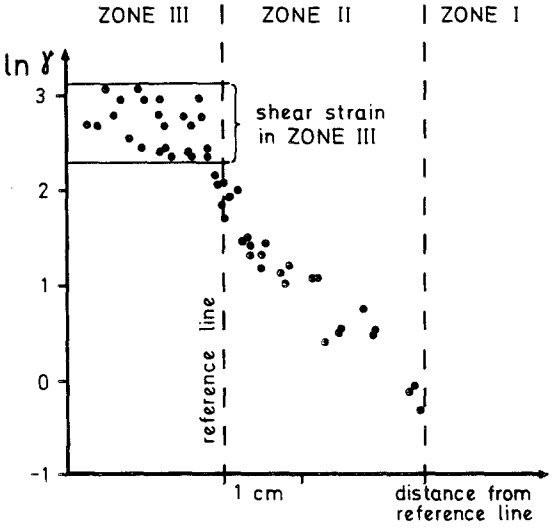

Fig.3c

Fig. 2. Small-scale shear zone in layered gabbroic and anorthositic rocks, shown as negative print to make the mylonitic foliation clearer. Scale bar is 5 cm long.

Fig. 3.(a) The sample cut perpendicular to the shear zone boundary and approximately parallel to the shear direction. Scale bar is 1 cm long, and the white bars indicate the orientation of the mylonitic foliation. (b) Location of the three structural and microstructural zones. The reference line is parallel to the shear zone boundary. (c) Shear strain profile based on the orientation of the mylonitic foliation (S_M).

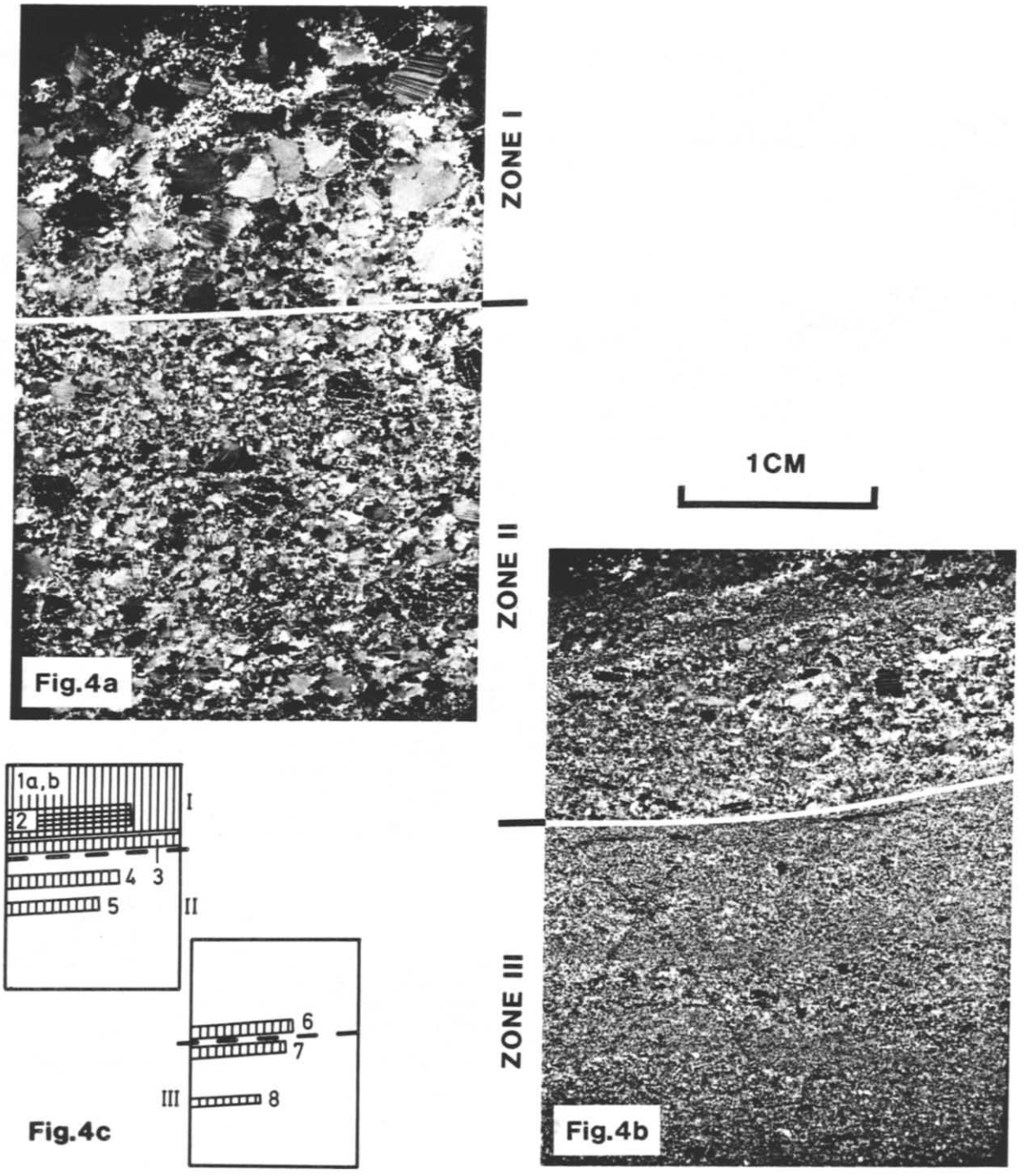

Fig. 4.(a) and (b) Micrographs of the two thin sections in their correct relative positions (cf. Fig. 3b) showing the microstructures in the three zones. (c) Areas of the two thin sections from which measurements of shape and indicatrix orientations of plagioclase grains were obtained: Samples 1–8 in the text and following figures.

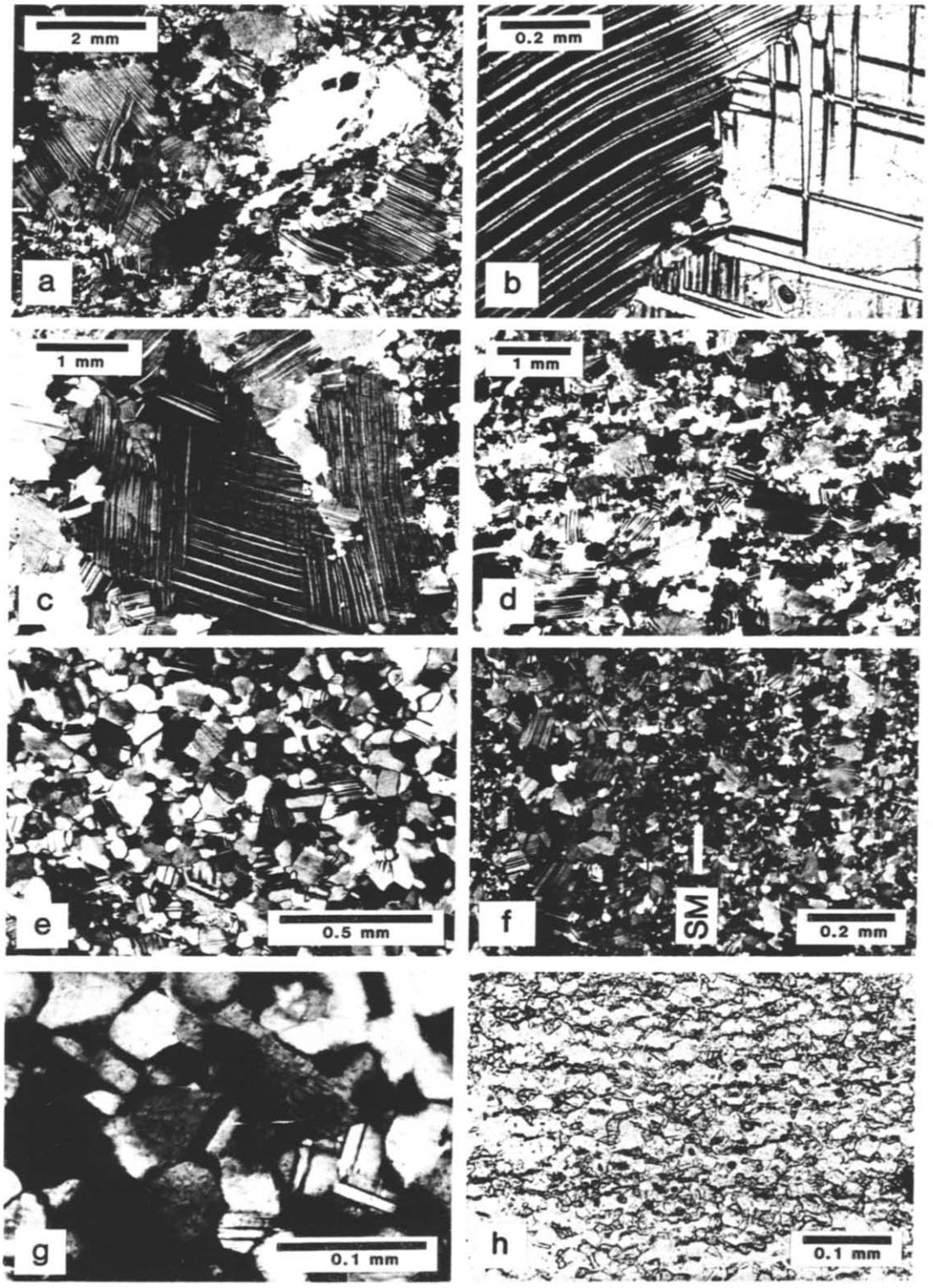

Fig. 5.(a) Typical microstructure outside the shear zone. Porphyroclastic texture of residual grains surrounded by festoons and multiple walls of new grains. (b) Two residual grains in zone I showing recrystallization on their mutual, lobate grain boundary. Note subgrain wall perpendicular to twinning in dark residual grain. (c) Deformed residual grain with embayment of recrystallized grains. (d) Inequigranular microstructure of lobate plagioclase grains in zone II. (e) Small recrystallized grains in zone II. (f) Typical microstructure in zone III. Mylonitic foliation (S_M) is defined by grain size variation of plagioclase between amphibole-free and amphibole-rich layers. (g) Small recrystallized grains in zone III. (h) Amphibole-rich layer in zone III where small amphibole grains are located on grain boundaries and at triple-junctions between plagioclase grains, or form a continuous network. Plane-polarized light.

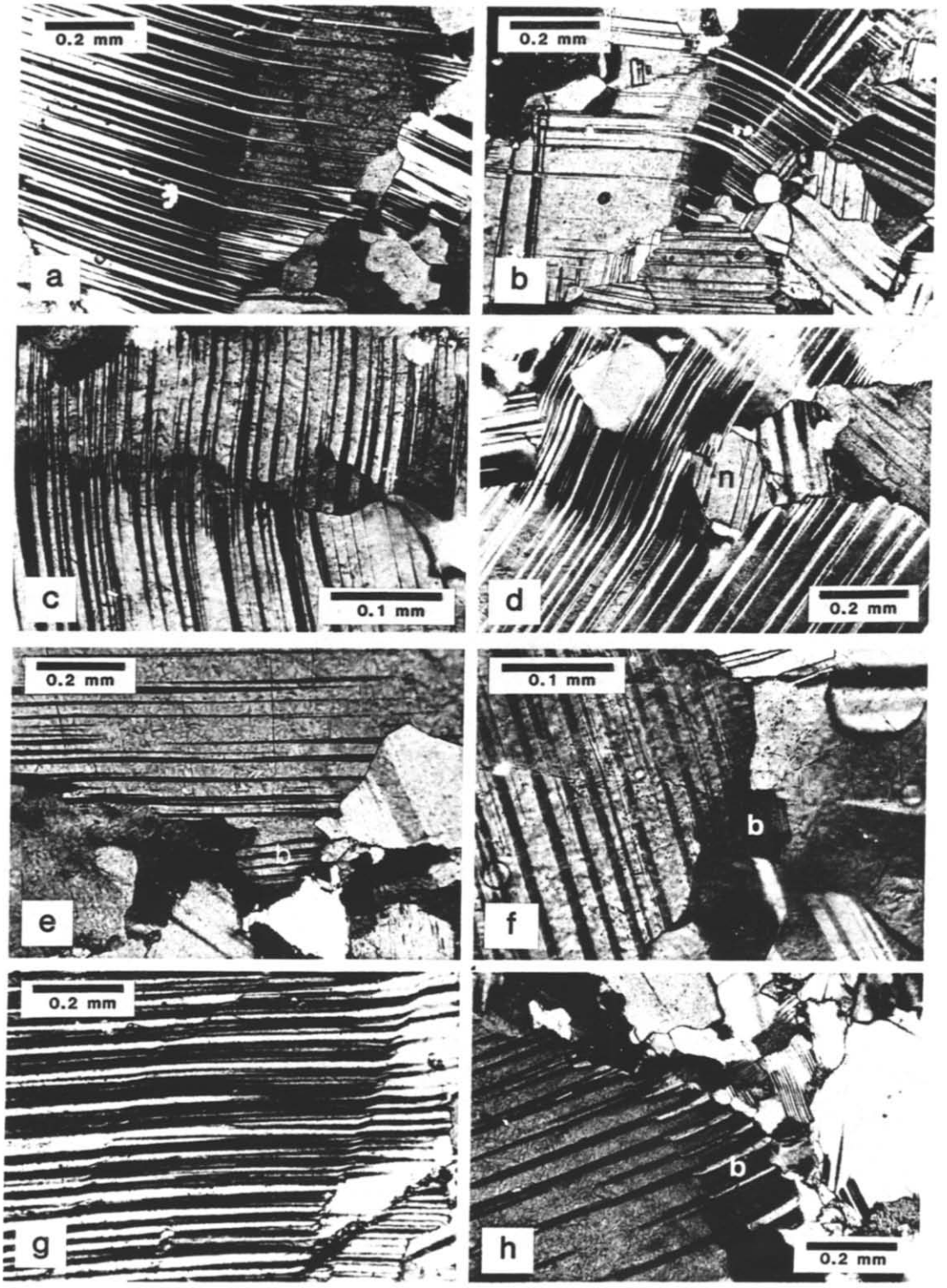

Fig. 6.(a) Plagioclase grain with some of the deformation twins terminating at a subgrain wall. (b) Bent and twinned plagioclase grain with subgrain walls perpendicular to the twinning. (c) Subgrain/new grain formed at a kink band boundary. (d) New grain (n) formed by subgrain rotation in a kink band. (e) A 'passive' bulge (b) formed where recrystallization leaves a bulge at a grain boundary. (f) 'Passive' bulge (b) separated from the host grain by a subgrain wall. (g) Plagioclase grain cut by narrow ductile shear bands. (h) A combination of shear zone deformation and subgrain rotation separates a potential new grain from its host. An incipient high-angle boundary is seen at the lower end of the shear band.

TABLE 1

(a) Modal content (%) of minerals in the sample

Plagioclase (An 68-78)	82.3
Amphibole	13.9
Garnet	2.9
Biotite, scapolite, chlorite	1.3
N (points): 4817	

(b) Modal content (%) of minerals in the structural zones

	zone I	zone II	zone III
Plagioclase	84	82	81
Amphibole	13	13	16
Garnet	2	4	2
Accessory	<1	1	2
N (points):	980	2362	1361

(c) Relative distribution of plagioclase twins in the structural zones (%)

	zone I	zone II	zone III
Plagioclase without twins	20	27	43
Plagioclase with one set of twins	57	49	43
Plagioclase with two sets of twins	23	24	14
N (points):	829	1945	1104

volume) large residual grains survive in zone II. 80% of the grains have a diameter between 0.1 and 0.5 mm, and most of these have formed by recrystallization of old grains. With increasing strain these grains acted as parent grains for further recrystallization. All grains with a diameter of more than 0.07–0.1 mm show evidence of strain and recrystallization to new grains with a diameter of 0.02–0.1 mm. These grains comprise 10–15% by volume, but this increases towards the centre of the shear zone. Their shape is equant to slightly elongate, with straight, curved or lobate boundaries (Fig. 5e). Only the larger grains show some evidence of strain, and about 40% are twin-free.

Zone III. The boundary between zone II and III is defined by a substantial decrease in the grain size of plagioclase (Fig. 4b). In zone III grain diameters range from 0.01 to 0.15 mm, with very few grains larger than 0.1 mm. Grains larger than 0.07 mm occur only in plagioclase-rich layers, whereas in the amphibole-rich layers the grain size is less than 0.05 mm (Fig. 5f). The larger grains are equant to slightly elongate with curved to lobate boundaries, many show evidence of strain and subgrains are common. These grains have recrystallized to very small grains (0.01–0.04 mm) with an equant shape and curved to straight boundaries. Only a few of these show evidence of strain, no subgrains were observed, and about 50% are twin-free (Fig. 5g).

Amphibole

In zone I, amphibole grains 0.1–1 mm in diameter form elongate aggregates, frequently with a garnet grain in the centre. The amphibole grains are equant to elongate with lobate to serrate grain boundaries; a few grains are fibrous. Only a few grains show subgrains and evidence of strain. With increasing strain, the amphibole has recrystallized to new grains with a diameter of 0.01–0.05 mm. The amphibole aggregates become more elongate and 'diluted' with plagioclase (zone II) and finally develop into amphibole-rich layers in zone III (Fig. 5h). These small amphibole grains are located on grain boundaries and at triple-junctions between plagioclase grains, or form a continuous network. This dissemination of minute amphibole grains has affected the recrystallization of plagioclase, since the plagioclase grains in layers rich in amphibole are much smaller than in amphibole-poor layers (Fig. 5f). Boullier & Gueguen (1975) suggested that this is evidence of superplastic deformation.

Plagioclase twinning

Only albite and pericline twins were found and both are polysynthetic. Point-counting of about 4000 grains shows that 70% are twinned, 49% have one set and 21% have two sets of twins. These figures are probably too low because twins with their composition plane subparallel to the thin section plane are not visible.

The morphology of the twins, the number of twins and the area of the grain affected by the twinning vary from grain to grain. Most twins cross the grain, some wedge-shaped twins terminate within the grain, and some spindle-shaped twins are completely contained within the grain. Twins can terminate at a subgrain boundary (Fig. 6a), indicating that the subgrain boundary was formed prior to or simultaneously with these twins.

The number of twin-free grains increases with decreasing grain size (Table 1c).

Recrystallization of plagioclase

Bulge nucleation and subgrain rotation (with or without coalescence) are often reported as the mechanisms responsible for the recrystallization of plagioclase (White 1975, Vernon 1975, Marshall & Wilson 1976). Both processes seem to have operated simultaneously in this shear zone, where lobate grain boundaries, subgrains, kink bands and evidence of recrystallization can be found in most grains larger than 0.07–0.1 mm.

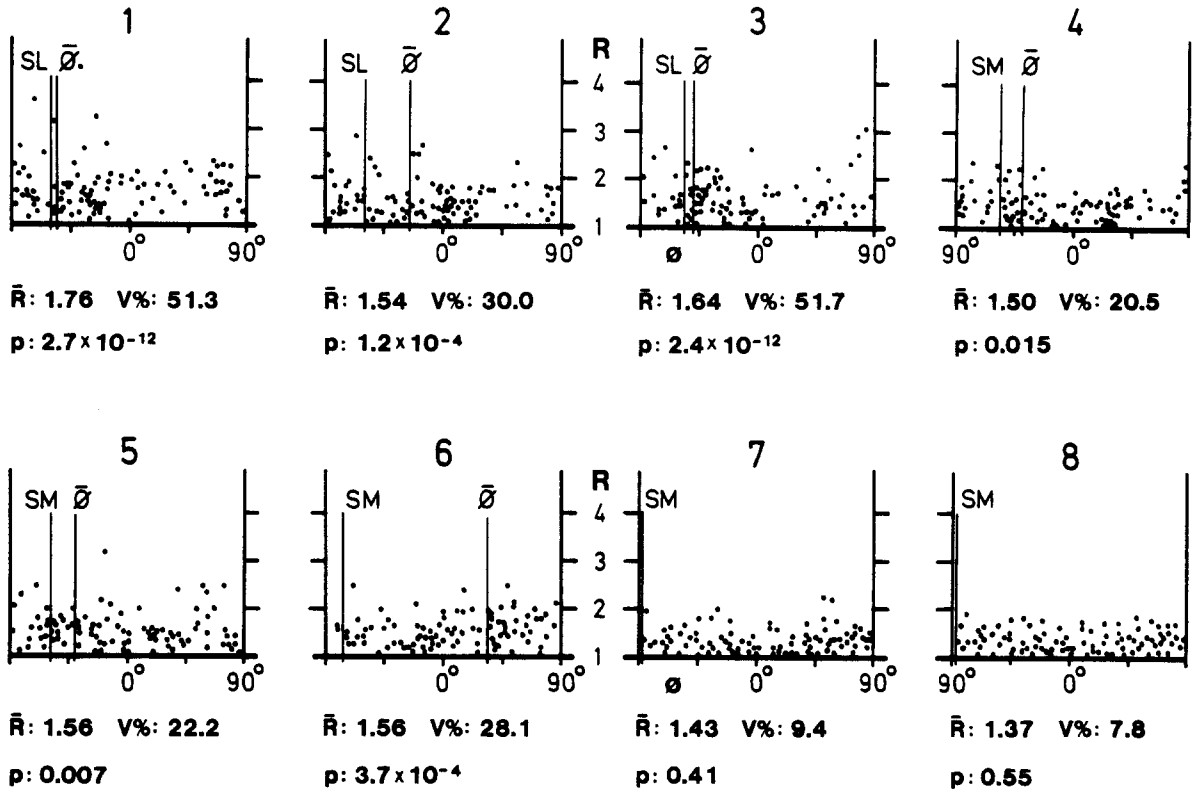

Fig. 7. R/ϕ plots of plagioclase grain shape fabric of the eight samples shown in Fig. 4c, $N = 100$ in each diagram. Sample 1 is old and sample 2 is new grains in zone I. S_L and S_M indicate the orientation of the foliation, and $\bar{\phi}$ is the mean orientation (resultant vector) of grain long axes. $\bar{R}$ is the mean aspect ratio of the grains. $V\%$ is the vector magnitude and P the probability as used by Jensen (1984). For $N = 100$, a R/ϕ distribution is regarded as significant when $V\% \geq 17.3$ and $P < 0.05$.

Subgrains are most commonly seen in bent and twinned grains (Fig. 6b) but they are also observed in twin-free grains. Where subgrains are present in a grain they are few in number and range from two larger (1–2 mm) subgrains which divide a residual grain to small subgrains (0.01–0.05 mm) along the grain boundary or kink bands (Fig. 6c). In twinned grains, subgrain walls are normally perpendicular to the twins (Figs. 6a & b). Larger subgrains have straight, curved or lobate boundaries, whereas smaller subgrains have straight to curved boundaries. New grains, inferred to have formed by subgrain rotation (Figs. 6c & d) thus vary in size from 0.01 to 2 mm. The upper limit depends on the size of the parent grain, whereas the lower limit may be due to the limited resolving power of the optical microscope and the thickness of a standard thin section.

Passive bulging where the grain boundary is bulged by recrystallization is very common (Fig. 6e). The size of bulges ranges from 0.03 to 0.1 mm and a subgrain wall commonly separates the bulge from the host grain (Fig. 6f). In such cases bulging and subgrain rotation must have cooperated as recrystallization mechanisms.

A third mechanism of recrystallization seems to have operated simultaneously with the mechanisms described above. A few grains are cut by one or a few narrow ductile shear bands (Fig. 6g) which divide the grain into two or more blocks (cf. Debat *et al.* 1978). If the shear deformation is combined with a relative rotation of the blocks, a high-angle boundary can form along the shear band and the block becomes a new grain. Figure 6h shows such a block (b) with an incipient high-angle boundary at one end of the shear band.

Host control

Recrystallization by subgrain rotation (Figs. 6c and d) is normally subject to host control, as demonstrated for plagioclase by Vernon (1975). In this case, however, general statistical evidence for host control is lacking. Measurements of the optical orientation of 159 recrystallized grains adjacent to two embayed residual grains in zone I yielded the data shown in Fig. 8, and these do not deviate significantly from the 'random' distribution curve presented by Ransom (1971), which actually shows a uniform distribution.

MICROFABRIC

Shape fabric

The shape fabric of plagioclase grains was analysed using a method described by Jensen (1984) and the results are presented graphically in Fig. 7. The average aspect ratio ($\bar{R}$) of the grains is between 1.37 and 1.76, generally decreasing with decreasing grain size. Grains in zone I and II have a significant shape fabric (vector magnitude $V \geq 17.3\%$ and $P \leq 0.05$) (Fig. 7, samples 1–6), whereas grains in zone III have a random orientation of grain long axes (Fig. 7, samples 7 and 8).

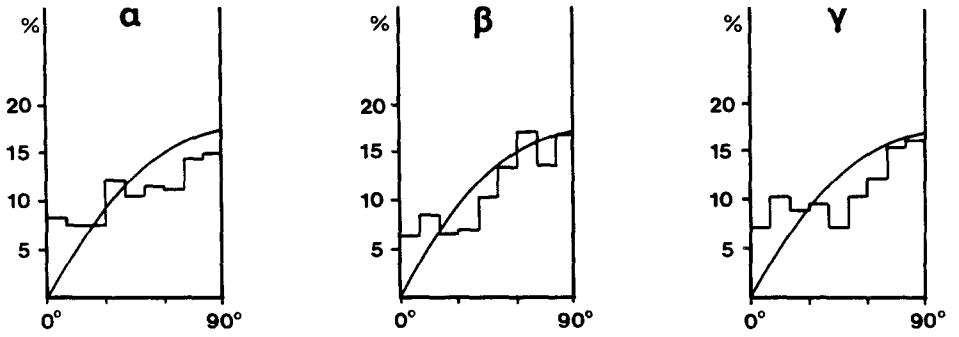

Fig. 8. Histograms of 159 measured angles between optical indicatrix axes of host and adjacent recrystallized grains for two embayed residual plagioclase grains in zone I. The 'random' distribution curve from Ransom (1971) is superimposed on each diagram.

Residual grains in zone I show a good shape fabric, with the long axes of grains parallel to the layering (S_L), Fig. 7, sample 1), whereas the new grains have a mean orientation of long axes ($\bar{\phi}$) deviating more than 30° from S_L (Fig. 7, sample 2). In zone II the misorientation between $\bar{\phi}$ and the foliation (S_M) is small close to zone I, but increases towards zone III, where the long axes of grains are randomly oriented. Thus, with decreasing grain size plagioclase grains develop lower aspect ratios and a dispersion in the orientation of long axes. In contrast, the mylonitic foliation becomes better defined with increasing strain.

Indicatrix fabric

The orientation of the optical indicatrix axes (α,β,γ) was measured using a 5-axis universal stage and the method described by Emmons (1943) and Möckel (1969). Orientation diagrams are presented in Fig. 9 and the sample locations are given in Fig. 4c. The method of Starkey (1977) has been used for plotting, contouring and statistical analysis of the data, and the statistical parameters of the orientation patterns are given in Table 2. These parameters are: (1) percentage of the area of the projection covered by zero point concentration (empty space) and (2) after dividing the data set into 10 subsets of equal size (n/10), M0% is defined as the mean percentage of empty space in these, with SD0% as standard deviation. The method of Allison *et al.* (1978) was used to evaluate whether the orientation data deviated significantly from a random distribution. No fabric is regarded as significant unless (M0 − 36.8%)/SD0% > 1, where 36.8% is the percentage empty space of a random distribution (Starkey 1977).

Zone I. Residual and new grains show similar orientation patterns (samples 1a and 1b, Fig. 9). The orientation pattern of the α axes is random, β axes lie in a poorly defined girdle (with maxima) parallel to the layering (S_L), and γ axes are concentrated near the pole to S_L. This concentration may form a partial girdle with point maxima 20–30° from the foliation pole (sample 1b). Sample 3 consists of 100 old and new grains and the orientation patterns are as described above.

Zone II. Modified versions of the orientation patterns described above are found in zone II (samples 4 and 5, Fig. 9). The α axes are randomly oriented; and the β axes lie in a girdle, with point maxima, parallel or sub-parallel to the foliation (S_M). In all samples the γ axes show the strongest point concentration. The pattern consists of elongated point maxima 20–30° from the pole to S_M, and these may fall on a small circle oblique to the foliation pole (sample 5). Sample 6 (Fig. 9) has a random orientation pattern. Thus the significant indicatrix fabric is lost somewhere between samples 5 and 6.

TABLE 2

Statistical parameters for the indicatrix orientation patterns shown in Fig.9

Zone	sample	n	axis	M0%	SD0%	random
I	1a	101	α	35.6	5.9	yes
		101	β	44.2	5.8	no
		101	γ	45.6	7.2	no
	1b	171	α	46.4	4.3	no
		171	β	45.8	4.8	no
		171	γ	50.2	7.2	no
	3	100	α	40.2	8.4	yes
		100	β	44.2	7.2	no
		100	γ	48.2	5.5	no
II	4	100	α	36.0	6.2	yes
		100	β	42.2	3.1	no
		100	γ	45.4	5.6	no
	5	100	α	40.2	9.4	yes
		100	β	42.2	4.0	no
		100	γ	46.7	7.8	no
	6	100	α	37.2	3.3	yes
		100	β	37.9	8.9	yes
		100	γ	40.5	8.5	yes
III	8	100	α	32.8	5.6	yes
		100	β	37.7	8.9	yes
		100	γ	37.1	7.1	yes

M0%: mean empty space %
SD0%: standard deviation on M0%
See text for further explanations.

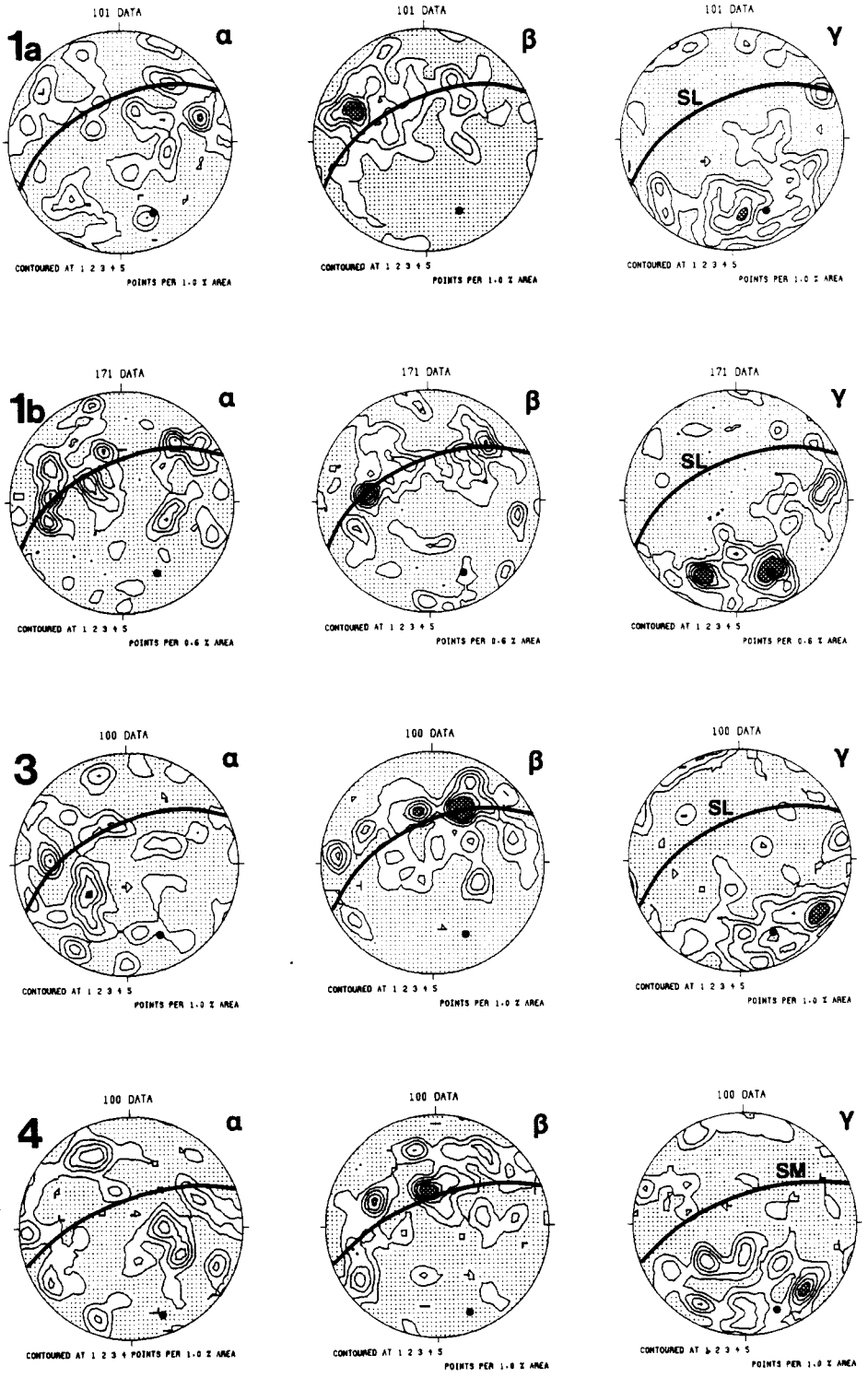

Fig. 9. (*Continued on facing page*).

Zone III. None of the indicatrix orientation patterns in the shear zone depart significantly from random (sample 8, Fig. 9).

In summary, the effect of the shear deformation on the fabric is as follows. With low to moderate strain (samples 3–5) a pre-existing indicatrix preferred orientation is slightly modified, but with higher strain this orientation pattern is destroyed.

Grains with their long axes within 30° from the foliation and a high aspect ratio ($R \geq 2$) were selected from samples 3–5 to see whether these grains have a special or more pronounced optical preferred orientation (cf. Mancktelow 1981), but this is not the case.

Crystallographic preferred orientation and inverse pole figures

A significant indicatrix fabric indicates a crystallographic preferred orientation, and knowledge of the crystallographic preferred orientation allows one to infer the possible dominant slip systems, assuming that the fabric was formed by intracrystalline slip (cf. Bouchez &

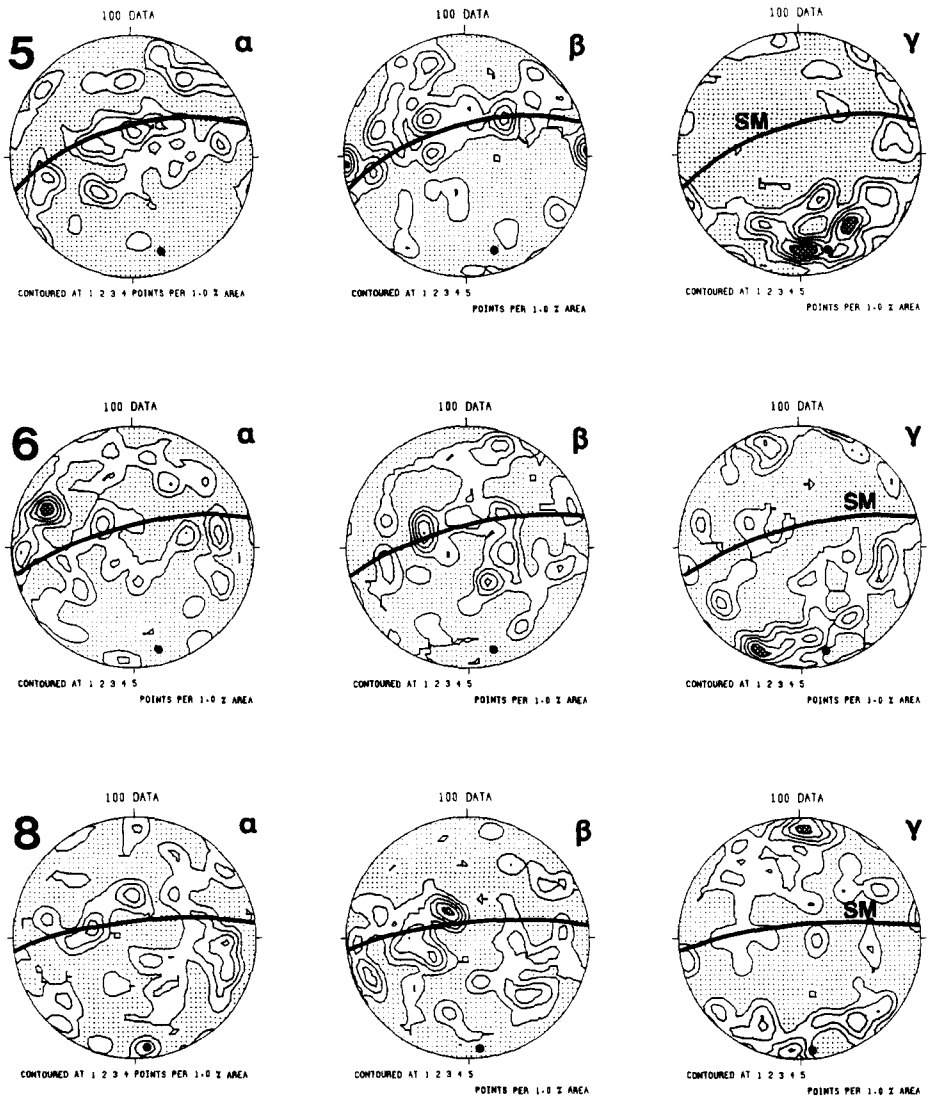

Fig. 9. Lower hemisphere equal-area plots of plagioclase indicatrix axes (α,β,γ). Orientation of the foliation (S_L, S_M) and the pole to the foliation is indicated in each diagram. The orientation of the reference plane (Fig. 3b) is E–W vertical and the shear direction is approximately E–W horizontal. The sample numbers correspond to those of Fig. 4(c). Sample 1a is residual grains, sample 1b is new grains and sample 3 is both old and new grains in zone I. Samples 4, 5 and 6 are from zone II and sample 8 is from zone III.

Lister 1983, Lister & Williams 1979). In previous work on plagioclase indicatrix fabrics (Crampton 1957, Shelley 1977, 1979) the authors used the fact that for a low anorthite content, the angles between indicatrix and crystallographic axes (a,b,c) are small. This however is not the case when the anorthite content is 68–78%, and we tried to overcome this problem in two ways, which will be illustrated using the orientation patterns of sample 5 (Fig. 9) as a typical fabric.

The first approach is to relate the measured indicatrix axes to crystallographic directions. For a given anorthite content an unique relation between indicatrix and crystal axes exists. This relationship is shown in diagrams published by Burri *et al.* (1967). Unfortunately, universal stage measurements of indicatrix ages do not indicate the positive or negative ends of the crystallographic axes. Thus, for a given indicatrix orientation there are four possible (symmetrical) orientations of a given crystal direction (Fig. 10a). A computer program was constructed to calculate these four orientations for each measured indicatrix orientation, and crystal orientation diagrams were constructed for eight crystallographic directions and poles to planes, namely a, b^*, c, $(\bar{1}11)$, (111), $(1\bar{1}0)$, (021) and $(\bar{1}12)$. Of these a, (111) and (021) gave significant preferred orientation patterns according to the criterion defined above (Figs. 10b–d). The (021) pole orientation pattern shows an enhanced version of the γ fabric (Fig. 9) indicating that the (021) plane is sub-parallel to the foliation (S_m). The a-axis orientation pattern shows a strong point-maximum in a poorly defined girdle sub-parallel to S_M. This may be an evidence for a slip system with glide in (021) sub-perpendicular to a, although such conclusions must be used with caution, since this method can create 'false' max-

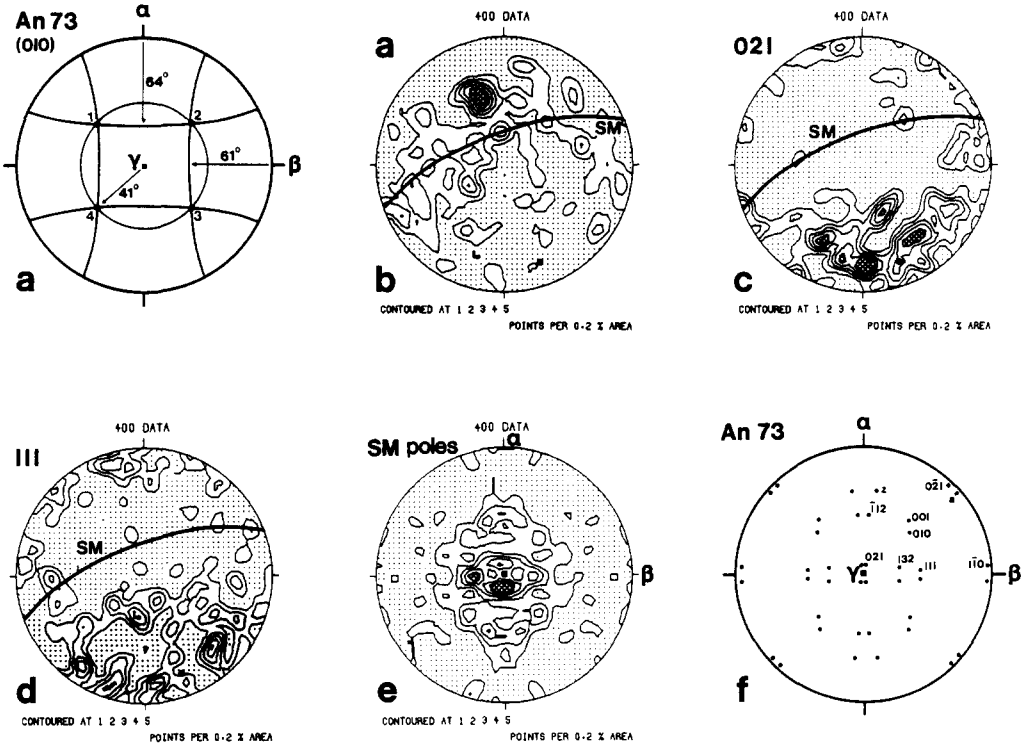

Fig. 10. Crystallographic orientation diagrams and inverse pole figure analysis using sample 5 (Fig. 9) as a typical fabric. (a) The four possible orientations of a crystallographic direction in relation to the measured indicatrix axes; pole to (010) used as an example. (b) Calculated a-axis orientation pattern. (c) Calculated orientation pattern for the pole to (021). (d) Calculated orientation pattern for the pole to (111). (e) Inverse pole figure illustrating the relations between the foliation pole and the measured indicatrix axes for sample 5. (f) Figure constructed to relate the inverse pole figure to crystallographic axes and poles to planes in plagioclase (An_{73}).

ima. After all, only one of the four possible orientations of a crystallographic direction is the real one.

The second approach is to construct an inverse pole figure (Tullis *et al.* 1973, Starkey 1979). For reasons mentioned above, there are four possible orientations of crystallographic directions and the foliation pole for a measured orientation of the indicatrix axes (Fig. 10a). An inverse pole figure for sample 5 shows a very strong concentration of the foliation pole close to γ and two strong maxima in the β–γ and the α–γ planes (Fig. 10e). Figure 10(f) was constructed to relate these maxima to crystallographic directions. One maximum is close to (021) and the other is close to (132). (021) has not been reported as a slip plane before (cf. Marshall & McLaren 1977, Scandale *et al.* 1983, Olsen & Kohlstedt in press) but Marshall & McLaren (1977) observed (13$\bar{2}$) as a slip plane in An_{77}. The foliation pole shows low concentrations close to the commonly reported (010) and (001) slip planes.

DISCUSSION AND CONCLUSIONS

The shear zone was formed during a high-grade metamorphic episode and shows no evidence of shear heating or post-tectonic recrystallization. The microstructures show that plagioclase in the shear zone was subject to dynamic recrystallization (Brown *et al.* 1980). With decreasing grain size, the grain aspect ratio decreases and grain boundaries become straighter. A finer grain size may cause a shift in the dominant deformation mechanism, from dislocation creep (with or without climb) to mechanisms controlled by grain boundary processes (White 1975, 1976, Boullier & Gueguen 1975). Destruction of the indicatrix fabric in the central part of the shear zone is probably the result of such a shift in dominant deformation mechanism, but whether the new mechanism was grain-boundary diffusion, grain-boundary sliding, superplastic flow, or some combination, (Boullier & Gueguen 1975, Allison *et al.* 1979) is not clear.

Boullier & Gueguen (1975) list six criteria for superplastic flow and five of these are satisfied in zone III: high temperature (>0.5 T_m), small grain size, a two phase 'alloy' of plagioclase and amphibole, equant grain shape and destruction of a crystallographic preferred orientation. However, this does not prove the operation of superplastic flow in zone III. Besides, the role of dynamic recrystallization as a possible deformation mechanism is as yet not fully understood.

Analysis of the crystallographic preferred orientation by use of crystal orientation diagrams and inverse pole figures (Fig. 10) suggests that (021) could be an operative slip plane with slip in the direction sub-perpendicular to a. Additionally planes close to (132) could be slip planes.

To overcome the (four-fold) ambiguity in construction of the crystallographic orientation diagrams (Fig. 10a), poles to albite and pericline twin planes and (001) cleav-

age could be measured, in addition to the indicatrix axes (cf. Suwa 1979). Unfortunately, such a procedure would be subject to a significant sampling control, since only 20–50% of the plagioclase grains show these features (Table 1c). A far better way out of this plagioclase fabric dilemma would be the combined use of X-ray fabric methods and inverse pole figures.

Acknowledgements—This work was supported by grants (to LNJ) from World University Service of Canada, the Danish Natural Science Research Council (grant No. 11-3859) and the Danish Ministry of Foreign Affairs. The sample and information about the geological context were most kindly provided by Niels Ø. Olesen. Thanks are given to colleagues at Statoil and Aarhus University for discussion and reading the manuscript. The paper has also benefited from constructive criticisms by the two anonymous reviewers.

REFERENCES

Allison, I., Kerrich, R. & Starkey, J. 1978. The variation of quartz orientation patterns in regional metamorphic tectonites. *Neues Jb. Miner. Abh.* **134**, 92–103.

Allison, I., Barnett, R. L. & Kerrich, R. 1979. Superplastic flow and changes in crystal chemistry of feldspars. *Tectonophysics* **53**, T41–T46.

Bouchez, J-L. & Lister, G. S. 1983. Fabric asymmetry and shear sense in movement zones. *Geol. Rdsch.* **72**, 401–419.

Boullier, A. M. & Gueguen, Y. 1975. Sp-Mylonites: origin of some mylonites by superplastic flow. *Contrib. Miner. Petrol.* **50**, 93–104.

Brown, W. L., Macaudiere, J., Ohnenstetter, D. & Ohnenstetter, M. 1980. Ductile shear zones in a meta-anorthosite from Harris, Scotland: textural and compositional changes in plagioclase. *J. Struct. Geol.* **2**, 281–287.

Bryhni, I., Brastad, K. & Jacobsen, V. W. 1983. Subdivision of the Jotun Nappe Complex between Aurlandsfjorden and Nærøfjorden, South Norway. *Norges geol. Unders.* **380**, 23–33.

Buddington, A. F. 1939. Adirondack igneous rocks and their metamorphism. *Mem. geol. Soc. Am.* **7**, 1–354.

Burri, C., Parker, R. L. & Wenk, E. 1967. *Die Optische Orientierung der Plagioclase*. Birkenhaüser, Basel.

Crampton, C. B. 1957. Regional study of epidote, mica and albite fabrics of the Moines. *Geol. Mag.* **94**, 89–103.

Debat, P., Soula, J-C., Kubin, L. & Vidal, J-L. 1978. Optical studies of natural deformation microstructures in feldspars (gneiss and pegmatites from Occitania, southern France). *Lithos* **11**, 133–145.

Emmons, R. C. 1943. The universal stage. *Mem. geol. Soc. Am.* **8**, 1–205.

Heim, M., Schärer, U. & Milnes, G. 1977. The nappe complex in the Tyin–Bygdin–Vang region, central southern Norway. *Norsk geol. Tidsskr.* **57**, 171–178.

Jensen, L. N. 1984. Quartz microfabric of the Laxfordian Canisp Shear Zone, NW Scotland. *J. Struct. Geol.* **6**, 293–302.

Kehlenbeck, M. M. 1972. Deformation textures in the Lac Rouvray anorthosite mass. *Can. J. Earth Sci.* **9**, 1087–1098.

Lister, G. S. & Williams, P. F. 1979. Fabric development in shear zones: theoretical controls and observed phenomena. *J. Struct. Geol.* **1**, 283–298.

Mancktelow, N. S. 1981. Strain variation between quartz grains of different crystallographic orientation in a naturally deformed metasiltstone. *Tectonophysics* **78**, 73–84.

Marshall, D. B. & Wilson, C. J. L. 1976. Recrystallization and peristerite formation in albite. *Contr. Miner. Petrol.* **57**, 55–69.

Marshall, D. B. & McLaren, A. C. 1977. The direct observation and analysis of dislocations in experimentally deformed plagioclase feldspars. *J. Mater. Sci.* **12**, 893–903.

Möckel, J. R. 1969. Structural petrology of the garnet–peridotite of Alpe Arami (Ticino, Switzerland). *Leid. geol. Meded.* **42**, 61–130.

Olsen, T. S. & Kohlstedt, D. L. 1984. Analysis of dislocations in some naturally deformed plagioclase feldspars. *Phys. Chem. Minerals.*

Ramsay, J. G. & Graham, R. H. 1970. Strain variation in shear belts. *Can. J. Earth Sci.* **7**, 786–813.

Ransom, D. M. 1971. Host control of recrystallized quartz grains. *Mineralog. Mag.* **38**, 83–88.

Scandale, E., Gandais, M. & Willaime, C. 1983. Transmission electron microscopic study of experimentally deformed K-feldspar single crystals. *Phys. Chem. Minerals* **9**, 182–187.

Shelley, D. 1977. Plagioclase preferred orientation in Haast schist, New Zealand. *J. Geol.* **85**, 635–644.

Shelley, D. 1979. Plagioclase preferred orientation, Forshore Group metasediments, Bluff, New Zealand. *Tectonophysics* **58**, 279–290.

Spry, A. 1969. *Metamorphic Textures*. Pergamon International Library, Oxford.

Starkey, J. 1977. The contouring of orientation data in spherical projection. *Can. J. Earth Sci.* **14**, 268–277.

Starkey, J. 1979. Petrofabric analysis of Saxony Granulites by optical and X-ray diffraction methods. *Tectonophysics* **58**, 201–219.

Suwa, K. 1979. Plagioclase twin laws and fabrics in three specimens of anorthosite. *Lithos* **12**, 99–107.

Tullis, J., Christie, J. M. & Griggs, D. T. 1973. Microstructures and preferred orientations of experimentally deformed quartzites. *Bull. geol. Soc. Am.* **84**, 297–314.

Vernon, R. H. 1975. Deformation and recrystallization of a plagioclase grain. *Am. Miner.* **60**, 884–888.

White, S. 1975. Tectonic deformation and recrystallization of oligoclase. *Contr. Miner. Petrol.* **50**, 287–304.

White, S. 1976. The effects of strain on the microstructures, fabrics and deformation mechanisms in quartzites. *Phil. Trans. R. Soc.* **A283**, 69–86.